To be presented at the International Conference on Narrow Gap Semiconductors (Colloque International CNRS: "Transition Semiconductor Semimetal") Nice, France, Sept. 10-12, 1973

LBL-2269

c.1

ELECTRONIC STRUCTURE OF NARROW GAP SEMICONDUCTORS

Marvin L. Cohen

September 1973

Prepared for the U. S. Atomic Energy Commission under Contract W-7405-ENG-48

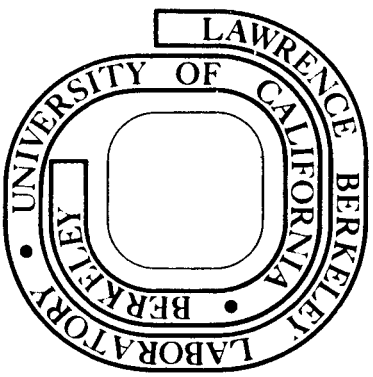

LBL-2269

c.1

DISCLAIMER

To be presented at the International Conference on Narrow Gap Semiconductors (Colloque International CNRS: "Transition Semiconducteur→ Semimetal") Nice, France, 1973.

Electronic Structure of Narrow Gap Semiconductors

Marvin L. Cohen*

Department of Physics, University of California

and

Inorganic Materials Research Division, Lawrence Berkeley Laboratory

Berkeley, California 94720

Abstract

Recent theoretical progress related to the one-electron theory of the electronic structure of several IV-VI and II-VI compounds and alloys are discussed. Some of the superconducting properties are also analyzed.

I. Introduction

Narrow gap semiconductors form a unique group of materials. The richness of the physical properties[1] of these compounds is probably unmatched by any other system of materials. In the IV-VI compounds alone, despite their simple structure, it is possible to observe ferroelectricity, superconductivity and laser action. The band structure effects[2] are extremely interesting; e.g. band edges invert, temperature coefficients of the gaps can be positive or negative, the Fermi surface

can be very complex, etc. From the point of view of device physics, narrow gap compounds are very important as these materials are used as detectors and generators of infrared radiation.

A large amount of work by talented researchers has helped to solve some of the problems related to the origin of the observed properties; however, some very basic questions about these semiconductors still remain unanswered. In this paper some of these questions will be discussed and the recent theoretical progress and problems in understanding the one-electron nature of these materials will be described. Some aspects related to superconductivity will also be discussed; however, other many-electron properties and device physics will not be explored. The majority of the description given here will be based on the use of the Empirical Pseudopotential Method[3] (EPM). Specific calculations concentrating on problems related to PbTe, PbSe, PbS, GeTe, SnTe, CdTe, HgTe and alloys of these materials are included.

II. IV-VI Compounds

The EPM band calculations for the lead salts,[4] SnTe[5] and GeTe,[5] and alloys of $Sn_x Pb_{1-x} Te$[6] are based on potentials obtained from analysis of other crystals (e.g. zincblendes). In most cases the optical constants such as reflectivity, $R(\omega)$, and modulated reflectivity $R'(\omega)/R(\omega)$ are in good agreement with experiment.[4] Using this data and the band calculations it is possible to obtain even closer agreement between experiment and theory by adjusting the pseudopotentials. However, such an adjustment is usually

unnecessary to obtain enough information to identify the principal optical structure.

The above procedure involves the use of local pseudopotentials. It is known[3] that the pseudopotential should be non-local to fit the energy levels over a wide energy range. In optical experiments, most of the transitions responsible for the prominent features arise from transitions between the upper valence and bottom conduction bands. In photoemission experiments like XPS (X-ray photoelectron spectroscopy) and UPS (ultraviolet photoelectron spectroscopy), it is possible to explore the lower valence bands. In these cases it is expected that the energies of the lower valence bands will not be in good agreement with experiment. Recent XPS studies[7] show that the calculated density of states spectra for the lead salts possess the basic structure seen in the experimental spectra, but the prominent structure is shifted. Considering the necessity of including d-wave potentials in germanium[8] and zincblende[9] materials and the d-character[2] of many of the levels in the lead salts, the inclusion of this type of non-local potential is almost certainly necessary to obtain agreement between photoemission experiments and the calculated valence band density of states.

Hopefully more complete calculations will be done to place the lower valence bands in the proper positions. However, at present, the situation is as stated above. The splitting between the upper valence bands and lower conduction bands are approximately correct and the lowest valence

bands are shifted in energy from the energies deduced from photoemission experiments. The general shapes appear basically correct.

What about states near the first band gap? Because of the particular nature of the band structure of the IV-VI compounds, studies of the structure in the uv and visible optical spectra don't give much information about the states near the band edge. Specifically, the separation between the top valence band and bottom conduction band is typically an order of magnitude larger than the energy of the fundamental gap. Therefore, calculations of the band structure which give accurate energy splittings in the uv won't necessarily yield the correct energies or ordering near the L point of the Brillouin zone where the fundamental gap occurs. It therefore remains the job of the experimentalist to determine the energy of the gap, the symmetries of the states at the gap, pressure coefficients, temperature coefficients and effective masses. Theoretical calculations can give a list of possibilities, however, and the results can be tested for consistency.

A good example of the type of dilemma possible occurs in PbTe. APW,[10,11] OPW[12] and EPM[4] band calculations give the following conduction band ordering L_6^- (L_2'); L_6^- (L_3'); L_{45}^- (L_3') whereas Bernick and Kleinman[13] using a modified pseudopotential scheme obtain L_6^- (L_3'); L_{45}^- (L_3'); L_6^- (L_2'). The energy differences here are small and it is possible to obtain either ordering by adjusting pseudopotential form factors in an EPM calculation.[14] Analysis of the results for the two orderings are shown to be inconclusive[14] when the results of the two calculations

are compared with experiment. Further study is needed to decide on the appropriate ordering.

The pressure and temperature dependence of the band edge states can be used to explore the nature of these states. In the lead salts, the pressure and temperature coefficients are positive whereas SnTe exhibits the more common negative coefficient behavior. Using measured compressibilities, Debye-Walter factors, Brook-Yu theory[15] and the EPM, good agreement with measured values can be obtained[16,17] for the pressure and temperature coefficients of the states near the band edge. The essential features of these calculations can be understood through some straightforward physical arguments associated with the energy band structure of the alloy series $Sn_x Pb_{1-x} Te$ (Fig. 1).

For PbTe, the maximum in the valence band is at the L point of the Brillouin zone with symmetry L_6^+. The conduction band minimum is also at L with symmetry L_6^-. The electronic charge density contours for the L states at the top of the valence band (Fig. 2a) clearly show that this state is p-like around Te and s-like around Pb. The charge density for the bottom conduction band (Fig. 2b) shows the reverse is true for this band. It is the p-like states which are affected most by the movement of the ions with temperature.[17] It is likely that this occurs because the movement of the ions about their equilibrium positions allows them to "feel" a larger change in charge density for the p-states than for the more constant s-states. In fact, it can be shown[17] that the temperature coefficients of the individual

states with p-like symmetry around a specific ion are linearly proportional to the mean square displacements of these ions. This implies that each level has a pressure or temperature coefficient associated with it.

Associating a pressure or temperature coefficient with a band state is not new or surprising. In the zincblende and diamond structure semiconductors this approach has been used to identify states; although to be more precise it is the pressure and temperature coefficients of energy differences that are usually considered. The feature in the $Sn_x Pb_{1-x} Te$ system that makes this approach seem unusual is that the levels being considered cross in energy. Near the reversal it is expected that the Fan[18] theory or band mixing would cause the band gap to decrease with temperature on the "Pb side" of the $Sn_x P_{1-x} Te$ alloy system. This doesn't happen. The L_6^+ and L_6^- states retain their identity and cross at L keeping the same signs for their temperature coefficients on the 'Sn side" as on the "Pb side." The details[17] are a bit complex, but the fact that L_6^- is now lower in energy than L_6^+ in going from Pb Te to SnTe means that the gap at L will decrease with higher temperature on the 'Sn side" rather than increase as it does on the "Pb side."

The above statements are true for the L point. An interesting feature of the SnTe band structure becomes apparent if the bands perpendicular to the Γ-L (Λ) direction are examined. In this case (Fig. 1), the bands cross away from L_1 and small gaps open where the unperturbed bands would have crossed resulting in a band edge away from the Λ-symmetry axis. Unlike PbTe, the minimum gap is therefore not at L, but slightly

away from L (Figs. 1 and 3). At and near the L point the arguments above would predict a negative temperature coefficient (i.e. $\partial E_g / \partial T < 0$). However, away from L past the crossing points of the two bands (perpendicular to Λ) the bands should retain the same character as in PbTe and the temperature coefficient should be positive. Tunneling measurements[19] which should explore states close to the minimum gap do give a negative coefficient. Optical measurements[20] examine states further away because of the Burstein shift caused by the Fermi level (see Fig. 3). These latter experiments yield a positive temperature coefficient. Both results are consistent with the band picture given here.

The details of the band structure near the edge needs further study. Refined transport studies should give a more precise description of the Fermi surface structure. Such work[21] is already giving a more detailed picture to test the theories.

At present there still isn't enough information to make final decisions on the band edge structure. Further theoretical work could help. Non-local EPM calculations with d-well potentials may give new possibilities for the form of the structure, but it appears unlikely at this point that the general features described here will change qualitatively. The prediction[5] by theory that the SnTe Fermi surface would be significantly different than PbTe has been confirmed by experiment. At this stage it is the detailed differences which must be explored.

The ionicity of the chemical bonds and the bonding nature of the zincblende and diamond materials has been explored[22,23] with much

success in recent years. Much less is known about the IV-VI compounds. Some features of the bonding can be explored through charge density plots for the valence band electrons (Figs. 4 and 5). As mentioned before, the valence bands, especially the lower ones are not given precisely by a local EPM, however the general features of the charge density should be correct. These calculations support ionic bonding rather than covalent bonding for PbTe; both have been proposed.[2]

Figure 4 displays the charge density contours for PbTe in the (1,0,0) plane for the sum of the five valence bands. The charge is concentrated about the non-metal (Te) site as is expected for six-fold rocksalt compounds. In Fig. 5, which contains the charge density in the $(1,\bar{1},0)$ plane, the chains of Pb-Te-Pb ... are displayed. Again the ionic nature of this material is evident. The chains appear to be molecular-like with ionic bonding between the elements.

It is interesting to compare the energy band structure of a typical IV-VI semiconductor (e.g. PbTe) with the diamond or zincblende series (e.g. Ge family). Some of the most obvious differences are the following. PbTe exists in the rocksalt structure, there are five filled valence bands, the maximum in the valence band is at L and the bonding is ionic. Ge crystallizes in the diamond structure, has four filled valence bands, the valence band maximum is at Γ and the bonding is covalent.

It is difficult to compare materials in different structures; however if the diamond structure is chosen and the potential of the atoms are

systematically varied, some interesting results are found. Such a model potential study has recently been done[24] for group IV materials. The pseudopotential was characterized by two parameters. One gave a measure of the repulsive core while the other represented the attractive region outside the core. Variation of these two parameters allowed the possibility of four types of band structures. If the attractive part of the potential is fixed near its Ge value and the repulsive core part is varied, the following results are obtained.

For a strong repulsive core, the band structure and charge density are essentially those of Ge. When the repulsive core potential is decreased, the gap between the top valence band and bottom conduction band decreases and becomes zero at one point in the Brillouin zone (the Γ point). The band structure is essentially that of grey tin and the charge density still shows covalent bonding. When the repulsive potential is decreased further (essentially to zero) a metal is obtained. The analogy would be Pb, but the crystal is forced to be in the diamond structure and not fcc. The charge density becomes spread out and metallic in nature.

From the point of view of the present study, the most interesting features occur when the core potential becomes attractive. Now the entire potential is attractive. A screened point ion-like potential was assumed, i.e. a Fermi-Thomas potential. This causes the electrons to pile up in the core region. Since the crystal is assumed homopolar, it is difficult to call the material ionic. However, a small antisymmetric potential

could be put in to account for two different atoms in a cell and then the ionic nature would be apparent.

The band structure for this system (Fig. 6) is very suggestive of PbTe. In the discussion above, the essential change which took place when the core potential was made less repulsive was the lowering of the s-like conduction band. In the Fermi-Thomas case this band has become so low in energy that it is now a low valence band. The first two bands are now s-like and low in energy. They do not contribute to the formation of sp^3 orbitals with the three higher p-bands. The result is <u>five valence bands</u> and a gap between the fifth valence band and the sixth band which is now the bottom conduction band.

The top valence band (Fig. 6) is very similar to the top PbTe valence band even though the crystal structure is different (but same Brillouin zone) and the model calculation is for a homopolar material. The maximum for the top valence band is at L with subsidiary maxima along Δ and Σ. This model calculation suggests that once the potential becomes sufficiently attractive, the s-states are practically core states; they dominate the charge density and bonding and sp^3 orbitals cannot be formed. For PbTe, the s-states are not as tightly bound as in the Fermi-Thomas model and the upper p-states do contribute to the bonding. The above results contrast the bonding nature of the IV-VI's and the Ge-like semiconductors. It would therefore be hazardous to attempt to apply the Phillips-Van Vechten[22] ionicity ideas and their ionicity scale to the IV-VI materials without substantial modifications.

The superconducting[25] properties of the IV-VI's are extremely interesting. GeTe and SnTe have been successfully tested and measurements of the dependence of the transition temperature, T_c, on carrier concentration have been performed. PbTe has been examined for a superconducting transition similar to SnTe and GeTe, but none has been found. This is probably because of the smaller density of states for the holes in this material compared with SnTe and GeTe.

Recently the Rennes[26] group have tested PbTe grown under unusual conditions. There appears to be a superconducting transition in these materials at very high temperatures. The authors of this work suggest that it is the Pb filaments which are superconducting in the PbTe matrix and propose that their results may be experimental verification of the existence of excitonic superconductivity.[27] Although Pb in PbTe is the typical system suggested[27] to test the excitonic superconductivity theory, this author believes that it is unlikely that these experiments confirm the excitonic theory. If the experiments are in fact correct and reproducible, then several alternate possibilities should be explored along with the excitonic mechanism.

Although it is a bit premature to discuss the details of the theory of the various explanations of these new experiments, it is worthwhile to speculate on the possible origins of the observed superconductivity (assuming the experiments are correct). The possibilities include superconducting Pb, highly doped PbTe and Te percipitates. In the Pb

case, excitonic superconductivity is possible, but not proven. McMillan's[28] equation with some harmless assumptions gives an estimate for the maximum superconducting transition temperature around 9K for Pb via electron-phonon interactions. The possibility of Pb having a higher T_c in another structure or in one dimensional-like filaments cannot be totally ruled out. One negative aspect of this latter suggestion is that Pb would probably still have a low Debye temperature in other structures and the maximum T_c would therefore be expected to be close to the 9K limit given above.

Highly doped PbTe is probably superconducting.[25] The transition temperature would depend on carrier density. Near the grain boundaries or on the surface, the PbTe could be highly doped. Since the bulk sample is[26] not superconducting, if PbTe itself were responsible for the observed superconductivity only a small amount of superconducting material would be consistent with the observed susceptibility. Using standard forms for the electron-phonon interactions, it appears that very high temperatures are not impossible but unlikely. A plausible estimate for the maximum T_c would be around 10K. New mechanisms are possible. Because of the larger variation of physical parameters possible in semiconductors, these materials appear to be more likely candidates for unusual mechanisms than the standard metals.

Te is another possibility. Te is superconducting[29] under pressure. The attractive aspect of Te is that it is normally a covalent semiconductor. In a metallic phase, it could still be "covalent-like" which is important[30] to high temperature superconductivity.

Another new series of experiments involving superconductivity and PbTe are being explored at Brookhaven National Laboratories.[31] Various superconducting metals are deposited in thin films on PbTe and enhancements of T_c are observed. In this case, again the possibility of superconductivity in the PbTe itself, Te, or Pb should be raised, and the above discussion could be modified to be applied to this case. Surface effects can be important here. Up to now, the transition temperatures are below 8K.[31]

It would be interesting to test SnTe and GeTe in the same manner as the Rennes and Brookhaven groups have examined PbTe. In these experiments if Te is responsible, similar results would be expected for SnTe and GeTe as for PbTe. If the metal or semiconductor represent the important ingredient, a change is expected. Since both SnTe and GeTe are superconductors, this type of experiment would be particularly interesting.

In the more conventional superconducting measurements in IV-VI materials, it appears that intervalley phonons coupling the degenerate valleys (Fermi surface pockets) can be used to explain the existing measurements. The same type of analysis has been applied to Sr TiO_3[25] although it is still not known with certainty that Sr TiO_3 does in fact have a many-valley conduction band. Experimental measurements indicate that this is the case, but band calculations[32] have raised the possibility of a single valley at Γ. The band calculations indicate that even at Γ

the Fermi surface would most likely have "arms" stretching out into the zone. If this were the case then large wavevector phonons could still be important.

Since GeTe, SnTe and Sr TiO_3 all have low frequency or soft phonon modes it is tempting to try[25] to associate the observed superconductivity with the soft phonons. Coupling directly to the TO modes[33] via the usual Frolich terms is not possible[25] and LO couplings get highly screened. Other couplings are possible[34] but for $SrTiO_3$ they have been shown to be small.[35] Coupling to two phonons is an interesting possibility which we had raised some time ago, but numerical estimates are discouraging.

If the intervalley phonons are assumed to dominate in SnTe and GeTe, the formulation for the electron-phonon coupling can be set up and a pseudopotential calculation of the intervalley phonon coupling constant can be performed. The coupling constants can also be extracted from fits to the experimentally determined curves for the transition temperature as a function of carrier concentration. The results are that the calculations[6,36] give values very close to the measured values.

Explorations of the role of other phonons and two phonon processes are still worthwhile since they may have a dominant role in other materials or their contributions in the cases of SnTe, GeTe and Sr TiO_3 may be measured.

III. $Cd_xHg_{1-x}Te$ Alloys

$Cd_xHg_{1-x}Te$ alloys form another interesting system with a variable energy gap. In CdTe the energy gap is 1.6 eV;[37,38] it decreases with Hg content and becomes zero around $x_c = 0.160 \pm 0.005$[39] (at low temperatures). For $x < x_c$ the gap becomes "negative" and it has a value of -0.30 eV[40] for $x = 0$ (HgTe).

The optical data[41] on both crystals allow an accurate EPM calculation[41] of the band structure and reflectivity. This calculation gave good agreement with the visible and uv data, but being a local EPM calculation, no attempt was made to fit the lower valence bands. A more recent non-local calculation[9] for CdTe gives the lower valence bands in good agreement with photoemission experiments. The uppermost valence band and lowest conduction band remain essentially the same as in the local EPM calculation.

Using the results of the local EPM calculation for CdTe and HgTe, it is possible to scale the potentials and lattice constant to examine[42] the electronic band structure of the alloy near the minimum gap at the Γ point in the Brillouin zone (Fig. 7).

The local EPM calculation[42] (Fig. 7) gives a cross-over position in excellent agreement with experiment. The energy gap is -0.01 eV at $x = 0.16$ and + 0.01 eV at $x = 0.17$. If the Γ_8 level is chosen as the reference energy, the essential feature which changes in going from HgTe to CdTe is the movement of the Γ_6 band. In HgTe, Γ_6 is below the top of the

valence band, Γ_8, giving the "negative" gap $E(\Gamma_6) - E(\Gamma_8) = -0.30$ eV. As x increases Γ_6 moves closer in energy to Γ_8, crosses and forms the bottom of the conduction band for $x > x_c$.

Motivated by the PbTe results discussed in the last section, the charge density for Γ_6 and Γ_8 was computed for both HgTe and CdTe[8] (Figs. 8 and 9). Because of degeneracy difficulties these charge density plots were made for points near Γ and not precisely at the Γ point. The interesting result is that the Γ_6 and Γ_8 states retained their identity, i.e. they had basically the same charge density contours, irrespective of whether the crystal was HgTe or CdTe.

The Γ_8 state is a p-like state centered around Te. It remains unchanged in going from HgTe to CdTe. The Γ_6 state is s-like with a high concentration around the Te site; it is approximately the same in both crystals. The charge is also s-like around the Hg and Cd sites for the Γ_6 state with some small differences; the Hg site has a higher concentration of charge than the Cd site.

On the basis of the success of the EPM to predict the cross-over point and to give accurate values for the band gaps and the fact that the Γ_6 and Γ_8 states retain their identity for both CdTe and HgTe, it was expected that a calculation of the temperature dependence of the energy gap should prove to be straightforward. This is not the case.

Using the same scheme as for the IV-VI materials it was found that the gap in CdTe had a negative temperature coefficient in agreement

with experiment, i.e. $|\partial E_g/\partial T| < 0$. Again following the arguments for the $Sn_xPb_{1-x}Te$ system, the temperature coefficient should change sign for HgTe. It does not. Theoretically one gets $|\partial E_g/\partial T| > 0$, while experimentally the result is $|\partial E_g/\partial T| < 0$.[43,44] In fact, the measured coefficient is negative until $x = 0.5$ and positive for $x > 0.5$. C. S. Guenzer and A. Bienenstock[45] have attempted similar calculations and have obtained essentially the same result. These authors suggest that the above problem is one of the major unsolved problems of semiconductor band theory and propose that the Brooks-Yu[15] theory which underlies the calculation of the temperature coefficient is inadequate.

Before making major changes in the theory it seems worthwhile at present to consider some of the detailed features for possible explanations. After all, the theoretical results are consistent with what one intuitively expects and with the $Sn_xPb_{1-x}Te$ results, i.e. the levels retain their temperature coefficients for all x. The charge density calculations give further support since these levels have similar distributions on the CdTe and HgTe sides of the alloy curve. This is particularly true for Γ_8. Therefore, the only apparent possibilities are that the Γ_6 and Γ_8 states do in fact change in going from CdTe to HgTe or the effect arises from the lattice change.

To explore the first possibility (the lattice effects have not as yet been investigated), calculations were done with a more attractive Hg potential. The optical spectra were computed and found to be in fair agreement with the measurements. The value for x_c was also found to be consistent with experiment and the temperature coefficient did

have the observed variation. The Fourier coefficients of the potential chosen did not have the standard monatomic increase for small reciprocal lattice vectors characteristic[3] of pseudopotential form factors. Because of this, the above exploratory calculation was not extended. In the standard EPM calculations, the potentials used are not too different from those calculated via model potentials.[3] The Hg potential obtained in the exploratory calculation did depart from the model potential; however, this departure may only be caused by the omission of non-local terms.

The above exploratory calculation did show that a calculation could probably be done which was consistent with all the data. The essential adjustment was to make the Hg potential more attractive. A speculation for the reason why this works is that a more attractive Hg potential would tend to extract charge from the Te ion causing the temperature coefficient of Γ_8 to decrease in magnitude.

If XPS or UPS data were to become available for HgTe, this will allow a fully non-local (d-wave) potential calculation for this material. Such a calculation together with CdTe calculations will hopefully solve the above problem. It is expected from other data[3] that the Hg and Cd non-local potentials should differ.

At this point further experiments on the band edges in the $Cd_xHg_{1-x}Te$ system would be very helpful. It is likely that a concentrated effort involving both experiment and theory is needed to solve the above problems even if the speculations and suggestions made here are correct.

Acknowledgement

I would like to thank D. J. Chadi, Y. W. Tsang and C. Varea de Alvarez for discussions and collaborations. Part of this work was done under the auspices of the U. S. Atomic Energy Commission.

References

* Supported in part by the National Science Foundation Grant GH 35688.

1. "The Physics of Semimetals and Narrow Gap Semiconductors," Edited by Carter and Bate, J. Chem. Phys. Solids 32 (Suppl. 1), 1971.
2. R. Dalven, Solid State Physics 28, 179 (1973).
3. M. L. Cohen and V. Heine, Solid State Physics 24, 37 (1970).
4. S. E. Kohn, P. Y. Yu, Y. Petroff, Y. R. Shen, Y. Tsang and M. L. Cohen, Phys. Rev. (in press).
5. Y. W. Tung and M. L. Cohen, Phys. Rev. 180, 823 (1969).
6. M. L. Cohen and Y. W. Tsang, J. Chem. Phys. Solids 32 (Suppl. 1), 303 (1971).
7. F. R. McFeely, S. Kowalczyk, L. Ley, R. A. Pollak and D. A. Shirley, Phys. Rev. B7, 5228 (1973).
8. J. C. Phillips and K. C. Pandey, Phys. Rev. Letters 30, 787 (1973). J. R. Chelikowsky and M. L. Cohen, to be published.
9. J. R. Chelikowsky, D. J. Chadi and M. L. Cohen, Phys. Rev. (in press).
10. J. R. Conklin, Jr., L. E. Johnson, and G. W. Pratt, Jr., Phys. Rev. 137, A1282 (1965).
11. S. Rabii, Phys. Rev. 167, 801 (1968).
12. F. Herman, R. L. Kortum, I. B. Ortenburg, and J. P. Van Dyke, J. Phys. (Paris) 29, C4-62 (1968).
13. R. L. Bernick and L. Kleinman, Solid State Comm. 8, 569 (1970).

14. Y. W. Tsang and M. L. Cohen, Solid State Comm. 9, 261 (1971).

15. C. Keffer, T. M. Hayes, and A. Bienenstock, Phys. Rev. B2, 1676 (1970). H. Brook and S. C. Yu (unpublished); see also S. C. Yu, Ph.D. Thesis, Harvard University, 1964 (unpublished).

16. Y. W. Tung and M. L. Cohen, Physics Lett. 29A, 236 (1969).

17. Y. W. Tsang and M. L. Cohen, Phys. Rev. B3, 1254 (1971).

18. H. Y. Fan, Phys. Rev. 82, 900 (1951).

19. L. Esaki and P. J. Stiles, Phys. Rev. Lett. 16, 1108 (1966); P. J. Stiles, J. Phys. (Paris) 29, 105 (1968).

20. J. R. Burke and H. R. Riedl, Phys. Rev. 184, 830 (1969).

21. R. S. Allgaier and B. Houston, Phys. Rev. B5, 2186 (1972); H. T. Savage, B. Houston and J. R. Burke Jr., Phys. Rev. B6, 2292 (1972).

22. J. C. Phillips, Rev. Mod. Phys. 42, 317 (1970).

23. M. L. Cohen, Science 179, 1189 (1973).

24. C. Varea de Alvarez and M. L. Cohen, Phys. Rev. (in press).

25. M. L. Cohen, "Superconductivity" edited by R. D. Parks, Marcel Dekker, Inc., New York, 615-644 (1969).

26. A. Lasbley, R. Granger and S. Rolland, to be published.

27. D. Allender, J. Bray and J. Bardeen, Phys. Rev. B7, 1020 (1973).

28. W. L. McMillan, Phys. Rev. 167, 331 (1968).

29. B. T. Matthias and J. L. Olsen, Phys. Lett. 13, 202 (1964).

30. M. L. Cohen and P. W. Anderson "Superconductivity in d and f band metals," ed. D. H. Douglass, Amer. Inst. of Physics, N.Y., p. 17 (1972).

31. D. L. Miller, B. Streetman, M. Strongin, and O. F. Kammerer, Bull. A.P.S. 18, 442 (1973); D. L. Miller, private communication.

32. L. F. Mattheiss, Phys. Rev. B6, 4718 (1972) and Phys. Rev. B6, 4740 (1972).

33. J. Appel, Phys. Rev. Lett. 17, 1045 (1966).

34. J. Appel, Phys. Rev. 180, 508 (1969).

35. P. B. Allen, Bull. A.P.S. 18, 327 (1973).

36. P. B. Allen and M. L. Cohen, Phys. Rev. 177, 704 (1969).

37. D. G. Thomas, J. Appl. Phys. 32, 2298 (1961).

38. W. G. Spitzer and C. A. Mead, J. Phys. Chem. Solids 25, 443 (1964).

39. C. Vérie, "Proceedings of the International Conference on II-VI Semiconducting Compounds" edited by D. G. Thomas (Benjamin, New York, 1967), p. 1124.

40. C. R. Pidgeon and S. Groves, in Ref. 39, p. 1080.

41. D. J. Chadi, J. P. Walter, M. L. Cohen, Y. Petroff, and M. Balkanski, Phys. Rev. B5, 3058 (1972).

42. D. J. Chadi and M. L. Cohen, Phys. Rev. B7, 692 (1973).

43. M. W. Scott, J. Appl. Phys. 40, 4077 (1969).

44. J. L. Schmit and E. L. Stelzer, J. Appl. Phys. 40, 4865 (1969).

45. C. S. Guenzer and A. Bienenstock, Phys. Rev. to be published.

Figure Captions

Fig. 1. Energy band structure near the L point in the Brillouin zone in directions parallel and perpendicular to the Λ axis at the L point for $Sn_xPb_{1-x}Te$ ($x = 0,\ 0.25,\ 0.5,\ 0.75,\ 1.0$).

Fig. 2. (a) Contours of constant charge density in the $(1,\bar{1},0)$ plane of PbTe for states in the top valence band at the L point. The charge density is plotted in units of e/Ω where Ω is the primitive cell volume. (b) Contours of constant charge density in the $(1,\bar{1},0)$ plane of PbTe for states in the bottom conduction band at the L point.

Fig. 3. Zero temperature band structure for SnTe near L for directions parallel and perpendicular to the Λ axis. Fermi levels, E_F, corresponding to various hole concentrations p are indicated.

Fig. 4. Contours of constant charge density in the $(1,0,0)$ plane of PbTe for the sum of the five valence bands. The units of charge density are (e/Ω) where Ω is the primitive cell volume.

Fig. 5. Contours of constant charge density in the $(1,\bar{1},0)$ plane of PbTe for the sum of the five valence bands. The units of charge density are e/Ω where Ω is the primitive cell volume.

Fig. 6. Energy band structure for a Fermi-Thomas model potential in the germanium crystal structure.

Fig. 7. Energy band structures, $E(\vec{k})$, near Γ for the alloy $Hg_{1-x}Cd_xTe$ ($x = 0,\ 0.16,\ 0.17,\ 1.0$). The $\vec{k}$-vector extends from Γ to $|\vec{k}| = 0.18\ (2\pi/a)$ in the Λ and Δ directions.

Fig. 8. HgTe charge densities near Γ for the Γ_8 conduction and valence levels (top), and the Γ_6 valence level (bottom).

Fig. 9. CdTe charge densities near Γ for the Γ_6 conduction level (top) and the Γ_8 valence level (bottom).

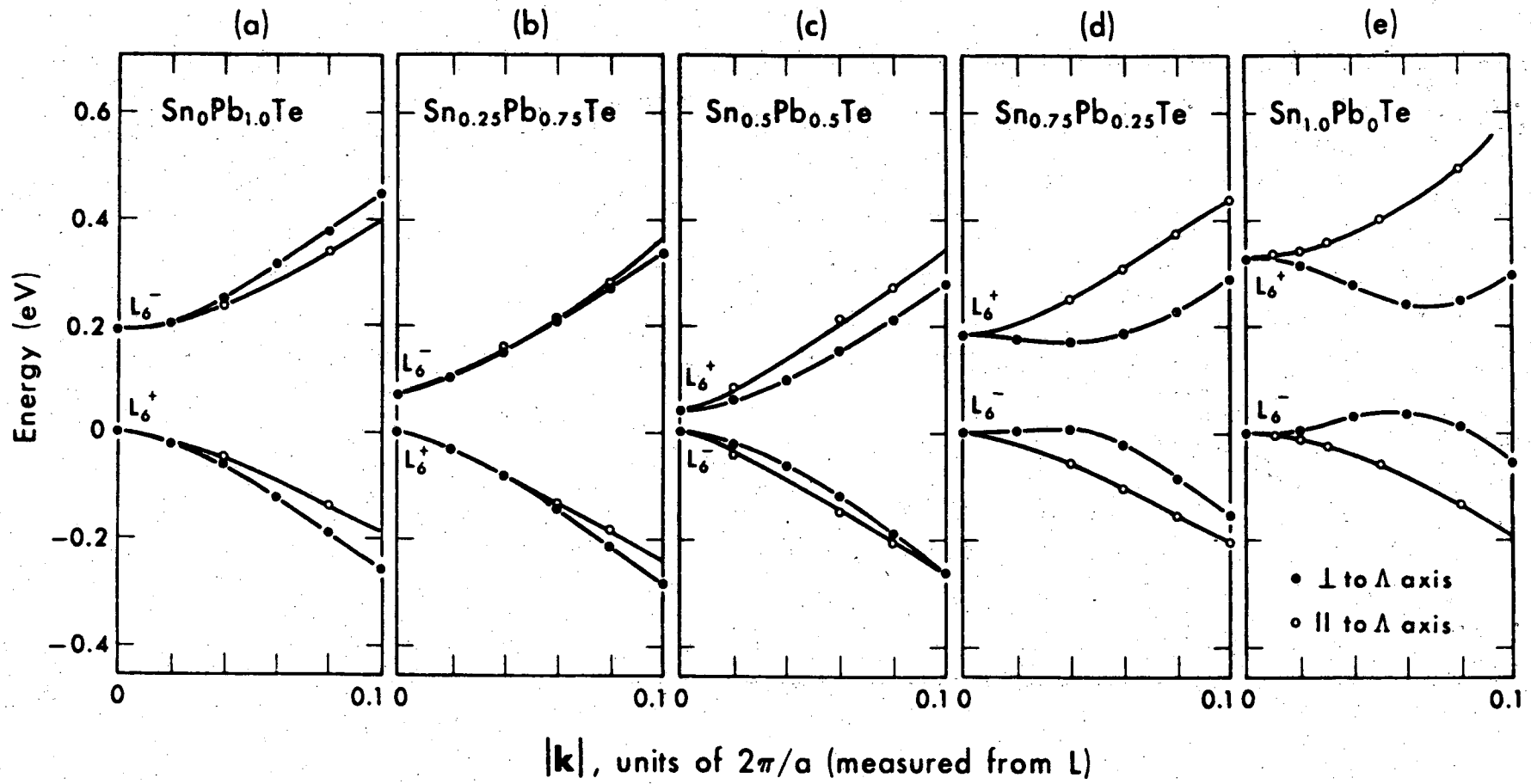
(a)
(b)
(c)
(d)
(e)
$Sn_0Pb_{1.0}Te$
$Sn_{0.25}Pb_{0.75}Te$
$Sn_{0.5}Pb_{0.5}Te$
$Sn_{0.75}Pb_{0.25}Te$
$Sn_{1.0}Pb_0Te$
L_6^-
L_6^+
Energy (eV)
0.6
0.4
0.2
0
−0.2
−0.4
0
0.1
• ⊥ to Λ axis
∘ ∥ to Λ axis
|k|, units of 2π/a (measured from L)

Figure 1

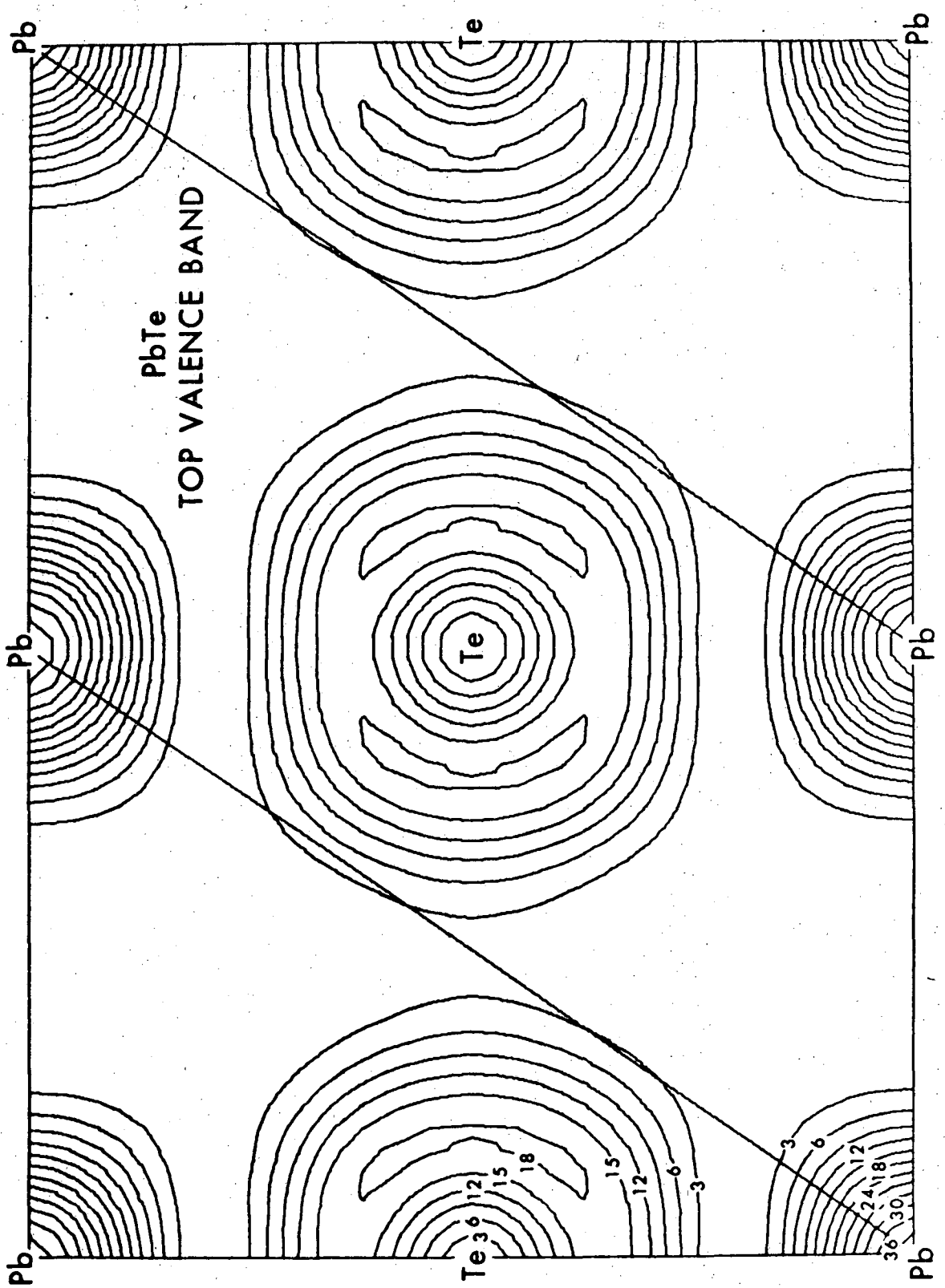
Pb
Te
Pb
PbTe
TOP VALENCE BAND
Pb
Te
Pb
Pb
Te
Pb
3
6
12
15
18
15
12
6
3
3
6
12
18
24
30
36

Figure 2a

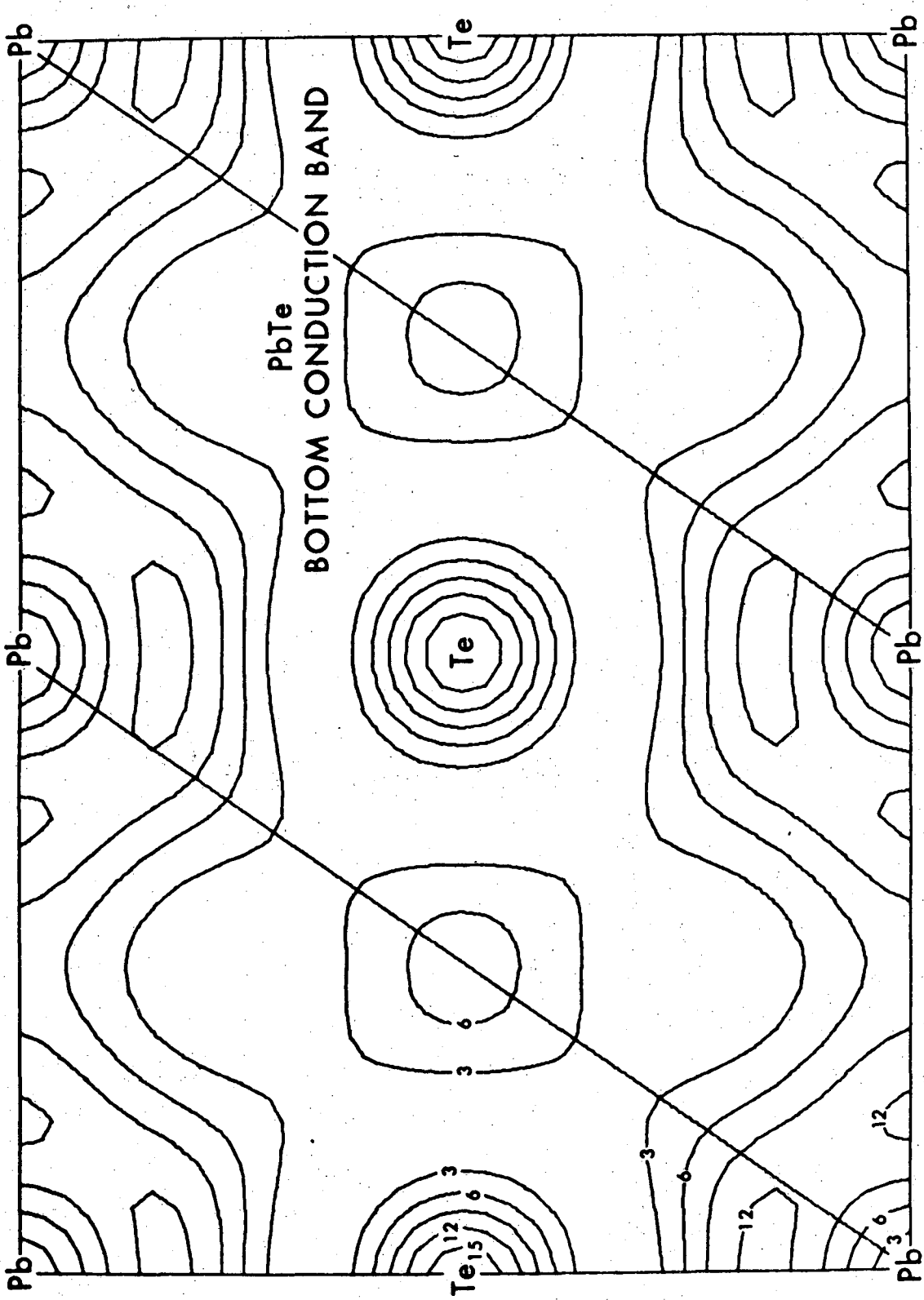
PbTe
BOTTOM CONDUCTION BAND
Pb
Pb
Pb
Pb
Pb
Te
Te
Te
0
3
3
6
12
15
3
6
12
3
6
12
3
6

Figure 2b

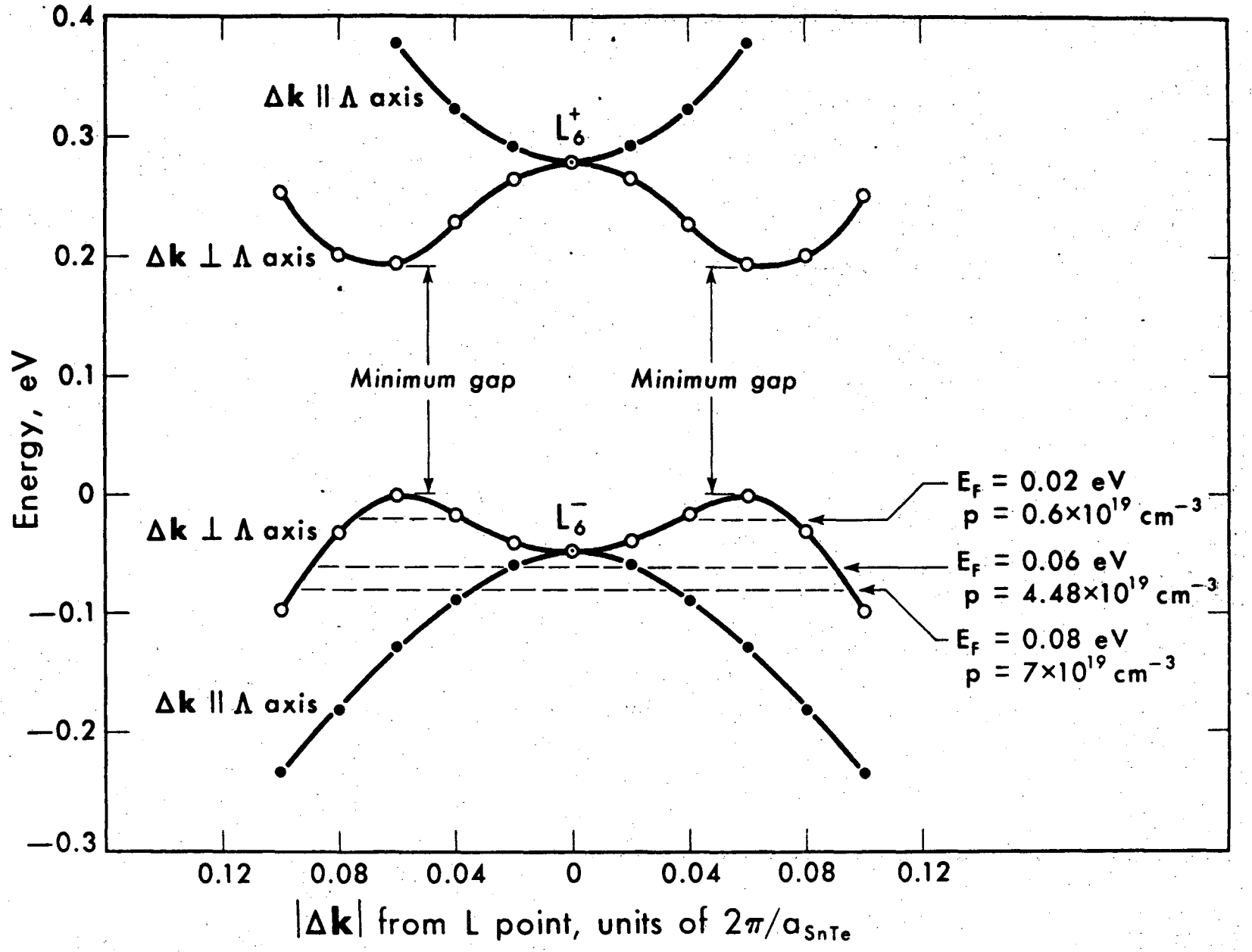
0.4
0.3
0.2
0.1
0
−0.1
−0.2
−0.3
Energy, eV
Δk ∥ Λ axis
L_6^+
Δk ⊥ Λ axis
Minimum gap
Minimum gap
Δk ⊥ Λ axis
L_6^-
Δk ∥ Λ axis
E_F = 0.02 eV
p = 0.6×10^19 cm^−3
E_F = 0.06 eV
p = 4.48×10^19 cm^−3
E_F = 0.08 eV
p = 7×10^19 cm^−3
0.12
0.08
0.04
0
0.04
0.08
0.12
|Δk| from L point, units of 2π/a_SnTe

Figure 3

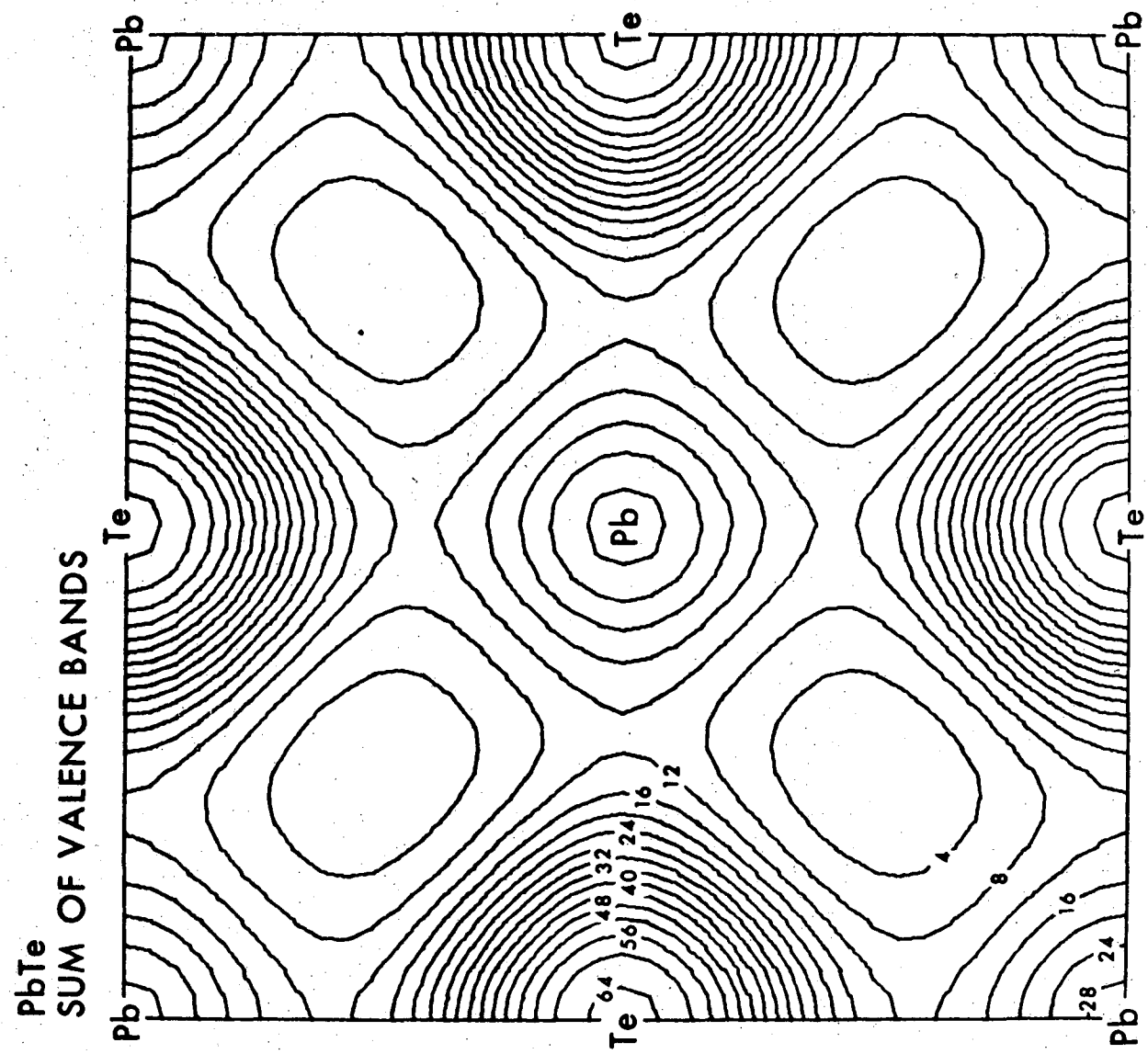
PbTe
SUM OF VALENCE BANDS
Pb
Te
Pb
Te
Pb
Te
Pb
Te
Pb
64
56
48
40
32
24
16
12
8
16
24
28

Figure 4

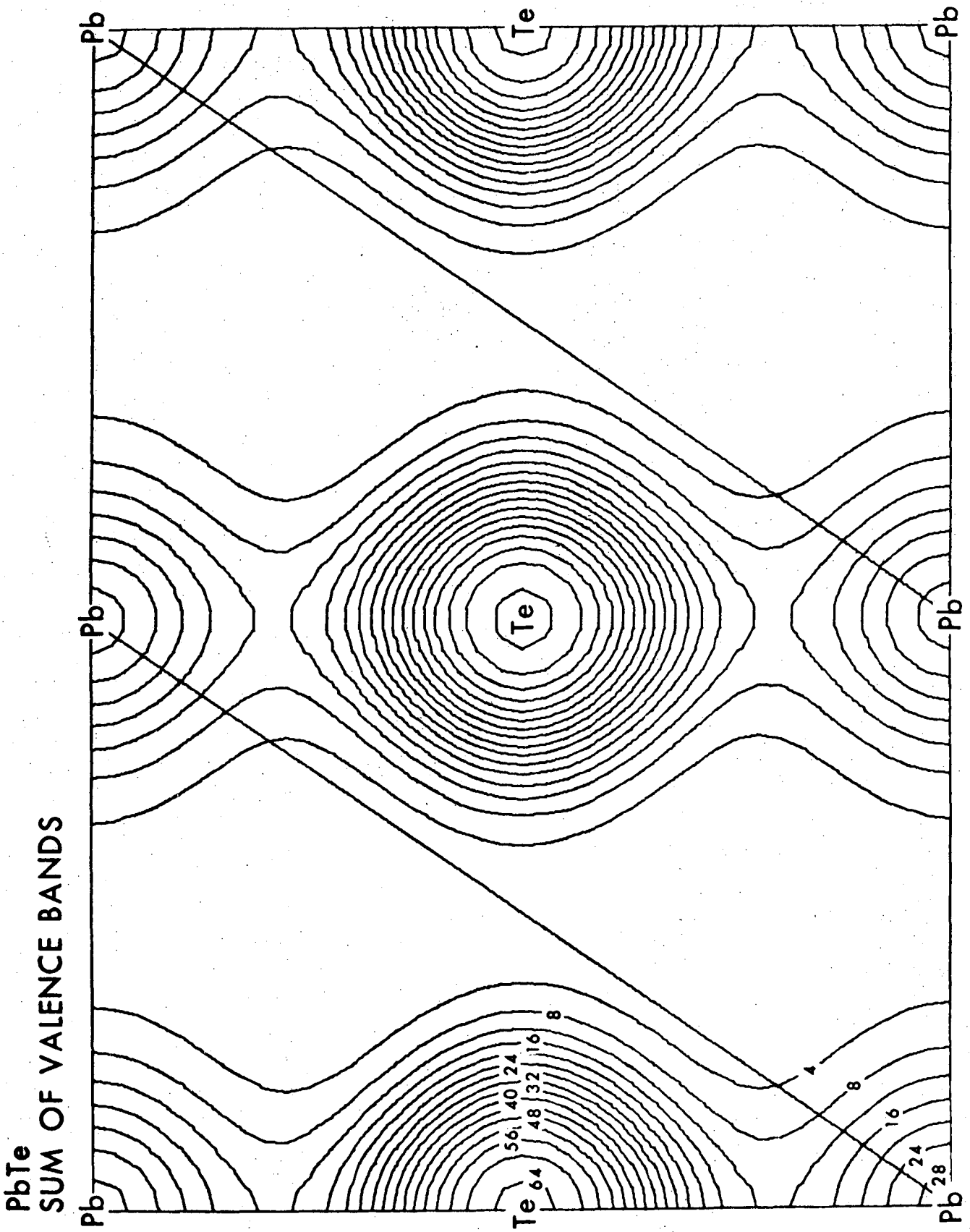
PbTe
SUM OF VALENCE BANDS
Pb
Te
Pb
Pb
Te
Pb
Pb
Te
Pb
64
56
48
40
32
24
16
8
4
8
16
24
28

Figure 5

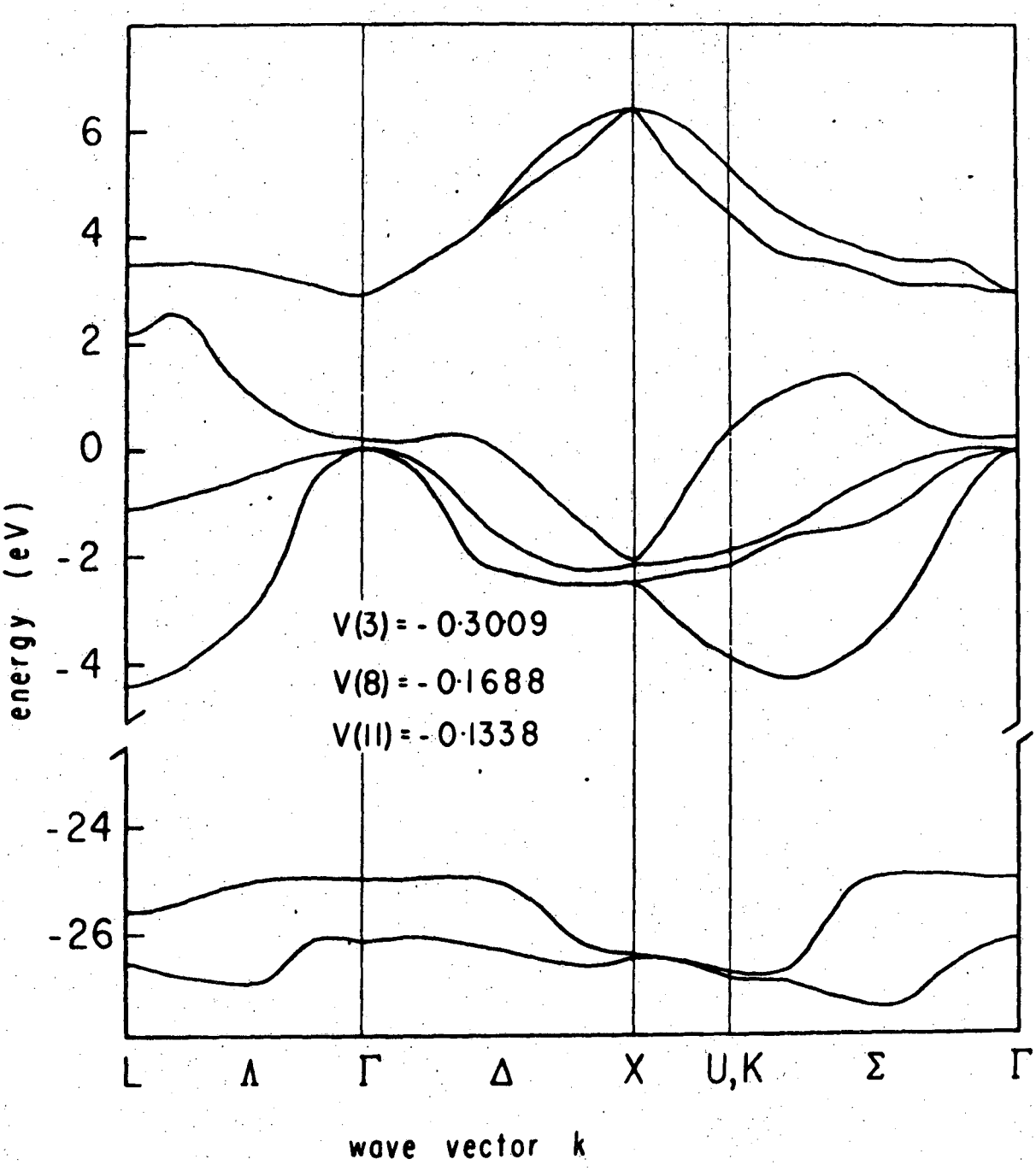
6
4
2
0
-2
-4
-24
-26
energy (eV)
V(3) = - 0·3009
V(8) = - 0·1688
V(11) = - 0·1338
L
Λ
Γ
Δ
X
U,K
Σ
Γ
wave vector k

Figure 6

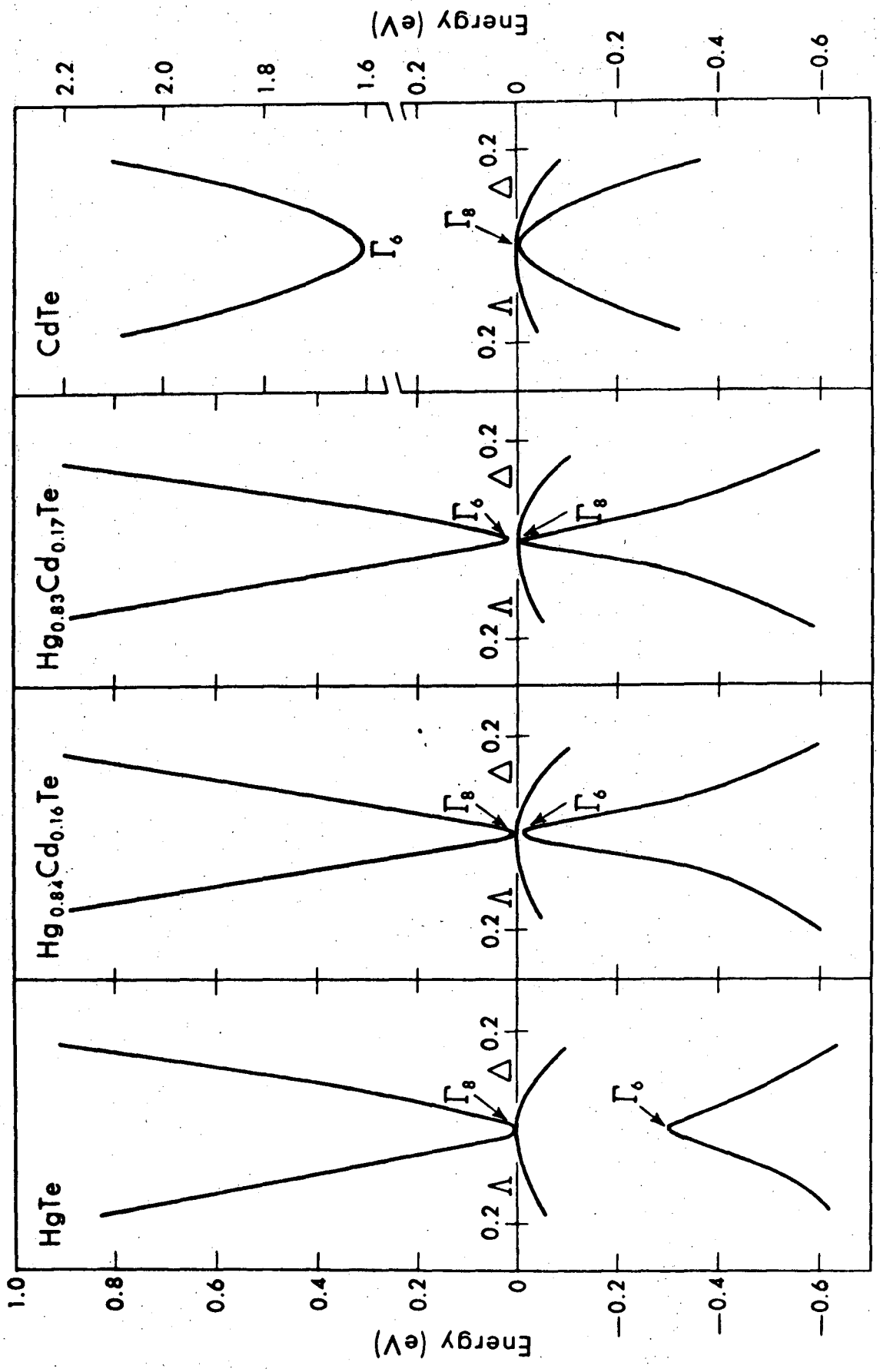
HgTe
Hg0.84Cd0.16Te
Hg0.83Cd0.17Te
CdTe
Γ6
Γ8
Δ 0.2
V 0.2
Energy (eV)
1.0
0.8
0.6
0.4
0.2
0
−0.2
−0.4
−0.6
2.2
2.0
1.8
1.6

Figure 7

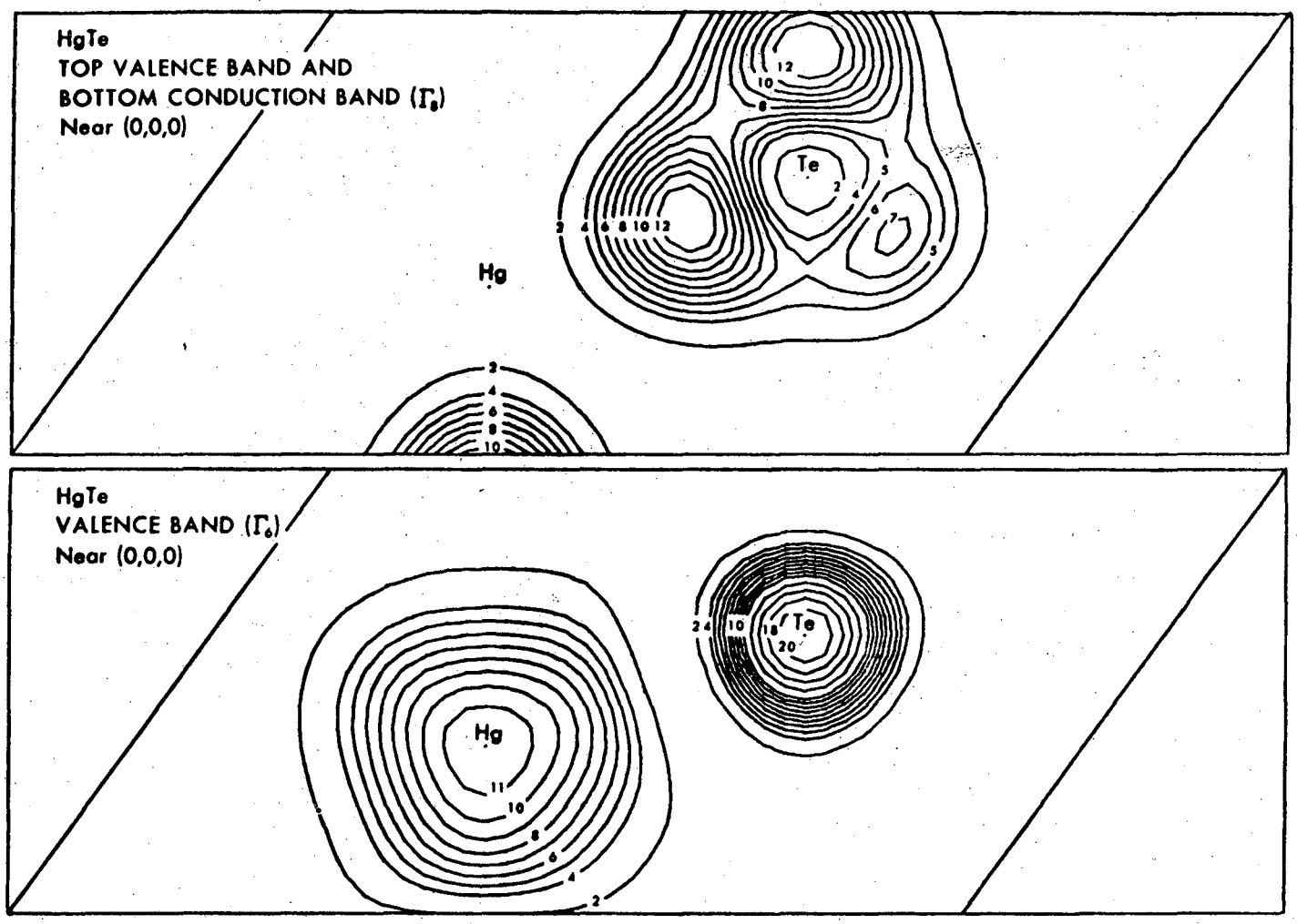
HgTe
TOP VALENCE BAND AND
BOTTOM CONDUCTION BAND (Γ_8)
Near (0,0,0)
Te
Hg
HgTe
VALENCE BAND (Γ_6)
Near (0,0,0)
Hg
Te

Figure 8

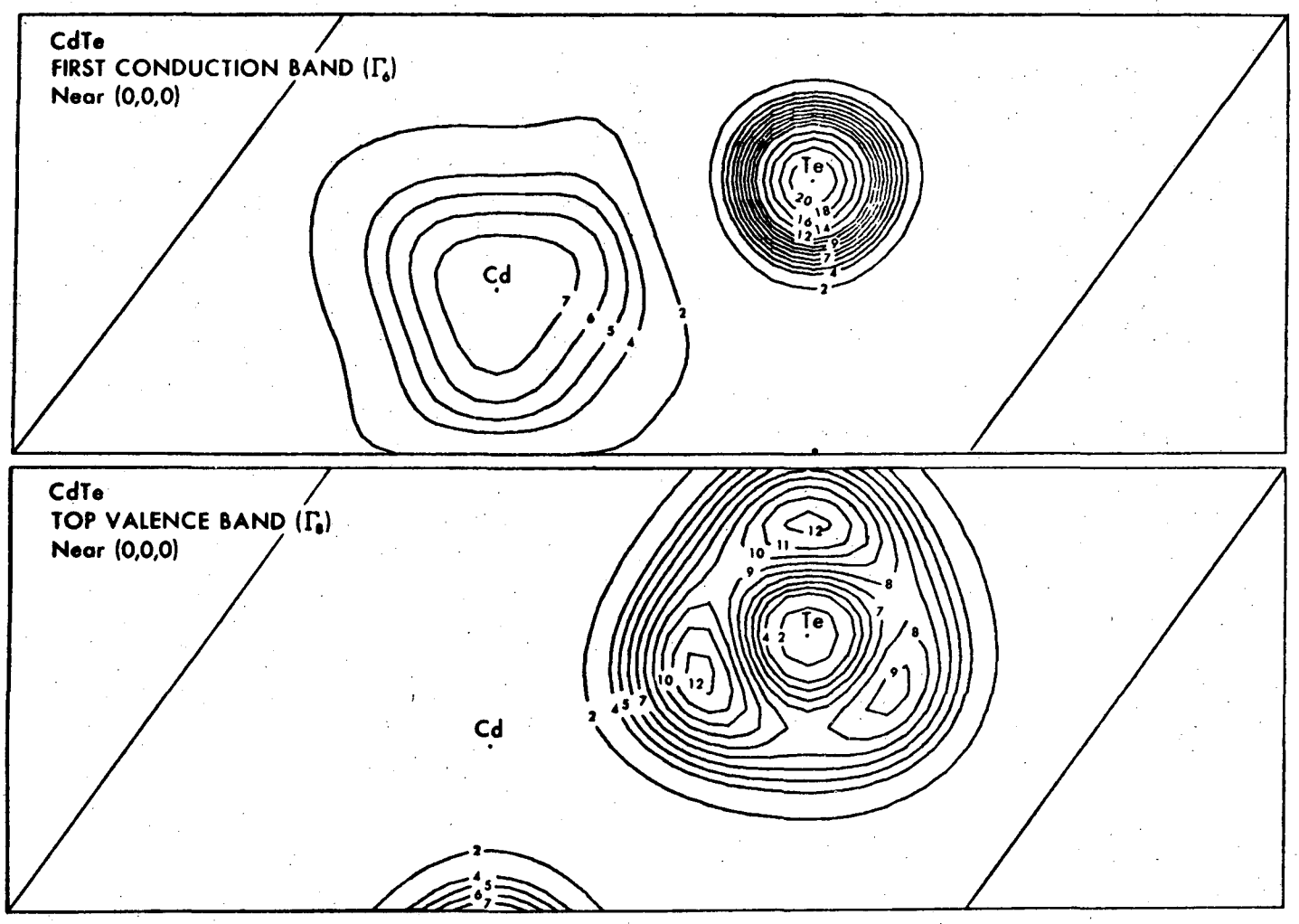
CdTe
FIRST CONDUCTION BAND (Γ_6)
Near (0,0,0)
Cd
Te
CdTe
TOP VALENCE BAND (Γ_8)
Near (0,0,0)
Cd
Te

Figure 9

TECHNICAL INFORMATION DIVISION
LAWRENCE BERKELEY LABORATORY
UNIVERSITY OF CALIFORNIA
BERKELEY, CALIFORNIA 94720